Eur. Phys. J. A **22**, 405–410 (2004)
DOI 10.1140/epja/i2004-10059-y

THE EUROPEAN PHYSICAL JOURNAL A

Saturation of nuclear matter and realistic interactions

Kh. Gad[a]

Physics Department, Faculty of Science, South Valley University, Sohag, Egypt

Received: 15 June 2004 / Revised version: 28 July 2004 /
Published online: 22 November 2004 – © Società Italiana di Fisica / Springer-Verlag 2004
Communicated by A. Schäfer

Abstract. In this communication we study symmetric nuclear matter for the Brueckner-Hartree-Fock approach, using two realistic nucleon-nucleon interactions (CD-Bonn and Bonn C). The single-particle energy is calculated self-consistently from the real on-shell self-energy. The relation between different expressions for the pressure is studied in cold nuclear matter. For best calculations the self-energy is calculated with the inclusion of hole-hole (hh) propagation. The effects of hh contributions and a self-consistent treatment within the framework of the Green function approach are investigated. Using two different methods, namely, G-matrix and bare potential, the hh term is calculated. We found that using G-matrix brought about non-negligible contribution to the self-energy, but this difference is very small and can be ignored if compared with the large contribution coming from particle-particle term. The contribution of the hh term leads to a repulsive contribution to the Fermi energy which increases with density. For extended Brueckner-Hartree-Fock approach the Fermi energy at the saturation point fulfills the Hugenholtz-Van Hove relation.

PACS. 21.65.+f Nuclear matter

1 Introduction

The evaluation of the saturation properties of nuclear matter from the basic nucleon-nucleon interaction has been extensively studied using the Brueckner-type resummation of ladder diagrams. The Brueckner-Hartree-Fock (BHF) definition of the self-energy has been extended to account for the effects of hh ladders in a perturbative way [1–4]. For a consistent treatment, however, one should treat the propagation of particle-particle (pp) and hh states in the in-medium scattering equation on the same footing. This turned out to be a rather ambitious aim. Starting from a single-particle propagator, which is characterized for each momentum k by one pole at the quasi-particle energy $\varepsilon_{\rm qp}$, only, the in-medium scattering reduces to the Galitskii-Feynman approach. If the hh part of the propagator is ignored, one obtains an equation for the ladder diagrams for the reducible two-particle Green function that corresponds to the Bethe-Goldstone equation. Using the complete Galitskii-Feynman propagator for nuclear matter at zero temperature with realistic NN interaction leads to the so-called pairing instability [5–7].

It has been argued [8] that it would be more natural to choose the propagator according to the Green function method, *i.e.* define the single-particle propagator with a single-particle energy which includes the real part of the self-energy as a single-particle potential for particle and hole states. This leads to a spectrum which is continuous at the Fermi momentum, which provided the name "continuous choice" for this approach. If, however, the single-particle potential, $U = 0$ is assumed above $k_{\rm F}$, then we have the conventional or gap choice. The continuous choice leads to an enhancement of the correlation effects in the medium and tends to predict larger binding energies for nuclear matter than the conventional choice. It is important to point out that, in the present communication we will focus our attention on the continuous choice. Also, we use exact Pauli operator to carry out our calculations.

Works using realistic interactions lead to a reasonable result for the saturation density and the binding energy at the saturation point. However, in violation of the Hugenholtz-Van Hove theorem, the resulting Fermi energy $E_{\rm F}$ at the saturation point is usually very different from the binding energy per particle E/N. Improvement of the fulfillment of the Hugenholtz-Van Hove property with respect to the G-matrix approximation is observed when using the quasi-particle T-matrix approach, or correction from hh [9,10].

It is known that the exact theory [11–13] should fulfill certain thermodynamical relations. We shall consider in the present work the equivalence of two ways of calculating the pressure in a system at zero temperature:

$$P = \rho^2 \frac{\partial (E/N)}{\partial \rho} \tag{1}$$

$$= \rho (E_{\rm F} - E/N), \tag{2}$$

[a] e-mail: kha92@yahoo.com

where ρ is the nuclear matter density. The relation between the Fermi energy and the binding energy at the saturation point is given by [11]

$$E_{\rm F} = E/N. \tag{3}$$

This equality of the Fermi energy and the binding energy per nucleon was derived by Weisskopf [14] on the basis of the independent particle model [15] which has been considered to be only a rough approximation. These relations are satisfied by the exact theory and can also be satisfied in a perturbative calculation to a given order of the expansion parameter. The realization of the above relation is very important, since it would give confidence to the single-particle properties obtained in the calculations.

Symmetric nuclear matter within the conserving, self-consistent T-matrix approximation has been studied [16–18]. This approach involves off-shell propagation of nucleons in the ladder diagrams. They found that the thermodynamic relations are well satisfied unlike for a G-matrix or a T-matrix approach using quasi-particle propagators in the ladders diagrams. Also they found that the full T-matrix and the G-matrix calculations give similar results for E/N using CD-Bonn and Nijmegen potentials [18]. Baldo and collaborators [19] obtained for the Argonne v_{14} potential [20] a saturation density corresponding to $1.565\,\mathrm{fm}^{-3}$ with about the correct amount of binding. This corresponds to an overestimation of the empirical density by about 60% but appears completely consistent with corresponding variational calculations [21] for the same potential. Gent group [22,23] studied the saturation of nuclear matter using a fully self-consistent treatment of short range. They found that the resulting saturation densities are closer to the empirical result when compared with (continuous choice) Brueckner-Hartree-Fock values. Arguments for the dominance of short-range correlations in determining the nuclear-matter saturation density are presented. It was argued in ref. [22] that the repulsive effect due to the inclusion of the hh scattering might be able to shift the saturation point close to the empirical value. Frick [24] studied the properties of symmetric nuclear matter at finite temperature using SCGF approach. He found that the Hugenholtz-Van Hove theorem is well fulfilled in the HF and the SCGF approximation, while it is badly violated in the BHF approach. He also gets on the saturation density in the SCGF approximation, $\rho_{\rm sat} = 0.31\,\mathrm{fm}^{-3}$. This value is still almost twice as large as the empirical saturation density ($\rho_0 = 0.17 \pm 0.02\,\mathrm{fm}^{-3}$).

Our main aim of the present communication is to investigate the relation between the binding energy and the Fermi energy taking into account different expressions for the pressure in cold nuclear matter with the Brueckner scheme and extended BHF (EBHF) approach. Throughout this paper two realistic NN interactions will be used and compared with other approaches. The present paper also contains further developments on the problem at hand. Finally, using two different ways, we shall calculate the self-energy for hh term.

2 Formalism

The integral equation for the Brueckner G-matrix is given by

$$\begin{aligned}\langle k_1k_2 \mid G(\omega) \mid k_3k_4\rangle &= \langle k_1k_2 \mid v \mid k_3k_4\rangle \\ &+\Sigma_{k_3'k_4'}\langle k_1k_2 \mid v \mid k_3'k_4'\rangle \times \frac{[1-\Theta_{\rm F}(k_3')][1-\Theta_{\rm F}(k_4')]}{\omega - \varepsilon_{k_3'} - \varepsilon_{k_4'}} \\ &\times\langle k_3'k_4' \mid G(\omega) \mid k_3k_4\rangle, \end{aligned}\tag{4}$$

where $\Theta_{\rm F}(k) = 1$ for $k < k_{\rm F}$ and zero otherwise. The product $Q(k,k') = [1-\Theta_{\rm F}(k)][1-\Theta_{\rm F}(k')]$, appearing in the kernel of eq. (4) enforces the scattered momenta to lie outside the Fermi sphere, and it is commonly referred to as the "Pauli operator". The G-matrix depends parametrically on the starting energy ω. The standard Brueckner approximation for the nucleon self-energy, has the following expression:

$$\begin{aligned}\Sigma^{\rm BHF}(k,\omega) &= \Sigma^{\rm HF}(k) + \Sigma^{\rm 2p1h}(k,\omega) \\ &= \Sigma_{k'<k_{\rm F}}\langle kk'|G(\varepsilon_k+\varepsilon_{k'})|kk'\rangle_{\rm A}\,,\end{aligned}\tag{5}$$

where ε_k is the self-consistent single-particle energy, label A means antisymmetrization, $\Sigma^{\rm HF}(k)$ is the Hartree-Fock self-energy (it is independent of energy) and $\Sigma^{\rm 2p1h}(k,\omega)$ is the self-energy for the two-particle one-hole (2p1h). In the BHF approach, (4) and (5) are solved self-consistently (for more information, see [3,25–29]).

The self-consistent Green-function (SCGF) approach differs in two main aspects from the BHF approximation. Firstly, within SCGF particles and holes are treated on an equal footing, whereas in BHF only intermediate particle states are included in the ladder diagrams. This aspect ensures thermodynamic consistency, *e.g.* the Fermi energy or chemical potential of the nucleons equals the binding energy at saturation (*i.e.* it fulfills the Hugenholtz-Van Hove theorem). In the low-density limit BHF and SCGF coincide. As the density increases the phase space for hh propagation is no longer negligible. Second, the SCGF generates realistic spectral functions, which are used to evaluate the effective interaction and the corresponding nucleon self-energy.

The contribution of the hh terms to the self-energy in a kind of perturbative way is given by [30,31]

$$\begin{aligned}\Sigma_G^{\rm 2h1p}(k,\omega) = &\int_{k_{\rm F}}^{\infty}\mathrm{d}^3p_1\int_0^{k_{\rm F}}\mathrm{d}^3h_1\,\mathrm{d}^3h_2 \\ &\times\frac{\langle k,p_1 \mid G \mid h_1,h_2\rangle^2}{\omega+\varepsilon_{\rm p_1}-\varepsilon_{\rm h_1}-\varepsilon_{\rm h_2}-i\eta}\,,\end{aligned}\tag{6}$$

which is graphically represented in fig. 1. If we take only the contribution coming from fig. 1b, in this case the self-energy for the hh term is given by

$$\begin{aligned}\Sigma_v^{\rm 2h1p}(k,\omega) = &\int_{k_{\rm F}}^{\infty}\mathrm{d}^3p_1\int_0^{k_{\rm F}}\mathrm{d}^3h_1\,\mathrm{d}^3h_2 \\ &\times\frac{\langle k,p_1 \mid v \mid h_1,h_2\rangle^2}{\omega+\varepsilon_{\rm p_1}-\varepsilon_{\rm h_1}-\varepsilon_{\rm h_2}-i\eta}\,.\end{aligned}\tag{7}$$

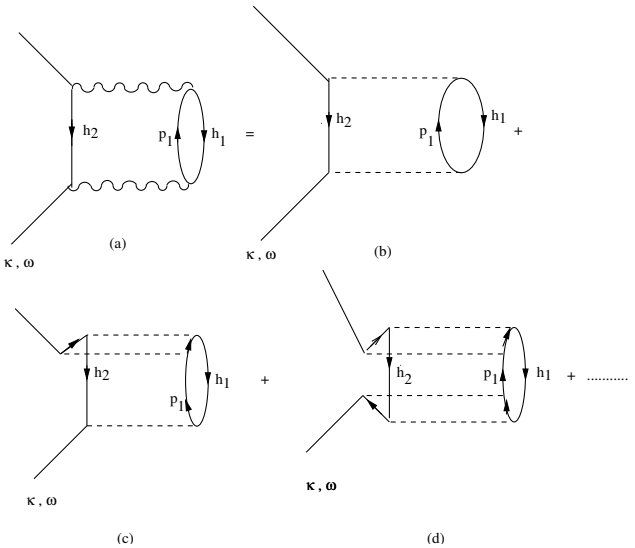

Fig. 1. Diagrammatic representation of the contribution two-hole one-particle Σ^{2h1p} to the self-energy and of the type of diagrams of the original perturbation series that it contains. An upward pointing arrow is associated with a particle state and a downward pointing arrow with a hole state. Horizontal dashed lines correspond to the antisymmetrized nucleon-nucleon interaction v and the wavy lines indicate the G-matrix.

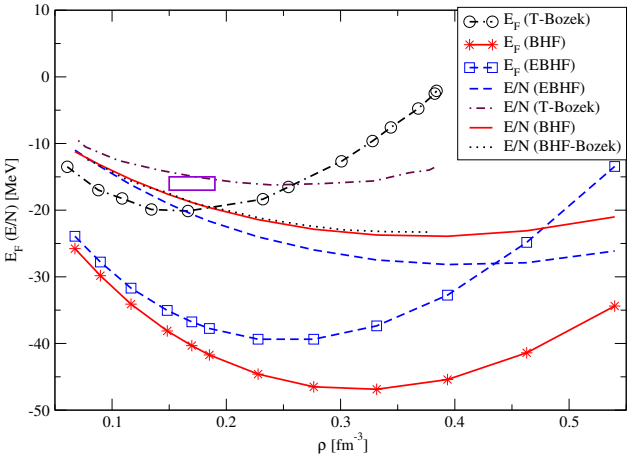

Fig. 2. The binding energy per nucleon and the Fermi energy as a function of the density ρ, all for the CD-Bonn potential. The binding energy for the BHF calculation (solid line), the BHF from ref. [18] (dotted line), the T-matrix calculation (dot-dashed line) [18] and the EBHF calculation (dashed line) are shown. The corresponding Fermi-energies results are denoted by the same lines with stars, squares and circles for the BHF, EBHF and T-matrix from ref. [18], respectively. The box indicates the empirical nuclear binding energy per nucleon.

Real and imaginary parts of the self-energy for two-hole one-particle (2h1p) are related to each other by a dispersion relation of the form [31]

$$\mathrm{Re}\,\Sigma^{2h1p}(k,\omega) = \frac{1}{\pi}\int_{-\infty}^{\infty}\frac{\mathrm{Im}\,\Sigma^{2h1p}(k,\omega')\mathrm{d}\omega'}{\omega'-\omega}\,. \quad (8)$$

The same is true also for the 2p1h.

Assuming that the self-energy for a nucleon in an infinite nuclear matter is given, the Dyson equation leads to a single-particle Green function of the form

$$g(k,\omega) = \frac{1}{\omega - \frac{k^2}{2m} - \Sigma(k,\omega)}\,. \quad (9)$$

If one compares this solution with the general Lehmann representation

$$g(k,\omega) = \lim_{\eta\to 0}\Bigg(\int_{-\infty}^{\varepsilon_F}\mathrm{d}\omega'\frac{S_h(k,\omega')}{\omega-\omega'-i\eta} + \int_{\varepsilon_F}^{\infty}\mathrm{d}\omega'\frac{S_p(k,\omega')}{\omega-\omega'+i\eta}\Bigg), \quad (10)$$

one can easily identify the spectral functions $S_h(k,\omega)$ and $S_p(k,\omega)$ for hole and particle strength, respectively [3].

In the EBHF approximation [3], we assume a single-particle spectrum $\tilde{\varepsilon}_k$ which is identical to the self-consistent BHF spectrum, but shifted by a constant C_1, which ensures the self-consistency for $k = k_F$

$$\begin{aligned}\tilde{\varepsilon}_{k_F} &= \varepsilon^{BHF}_{k_F} + C_1 \\ &= \frac{k_F^2}{2m} + \Sigma^{BHF}(k_F,\omega=\tilde{\varepsilon}_{k_F}) \\ &\quad +\Sigma^{2h1p}(k_F,\omega=\tilde{\varepsilon}_{k_F}).\end{aligned} \quad (11)$$

The constant C_1 is indeed just a constant shift to account for the contribution of the 2h1p term in the self-energy. It is calculated in a self-consistent manner from relation (11). It is used only for the redefinition of the single-particle spectra in the Bethe-Goldstone equation and the 2h1p term. It has been introduced to avoid a complete recalculation of the self-energy.

This shifted single-particle spectrum is also used in the Bethe-Goldstone equation. Also the quasi-particle energy is given by

$$\begin{aligned}\varepsilon_{qp}(k) &= \frac{k^2}{2m} + \Sigma^{BHF}(k,\omega=\varepsilon_{qp}(k)) \\ &\quad +\Sigma^{2h1p}(k,\omega=\varepsilon_{qp}(k)).\end{aligned} \quad (12)$$

The total energy per nucleon for EBHF is calculated as

$$\frac{E}{A} = \frac{\int \mathrm{d}^3k \int_{-\infty}^{\varepsilon_F}\mathrm{d}\omega\, S_h(k,\omega)\frac{1}{2}\left(\frac{k^2}{2m}+\omega\right)}{\int \mathrm{d}^3k\, n(k)}\,. \quad (13)$$

3 Results and discussions

Figure 2 shows the binding energy in the different approaches as a function of the density in symmetric nuclear

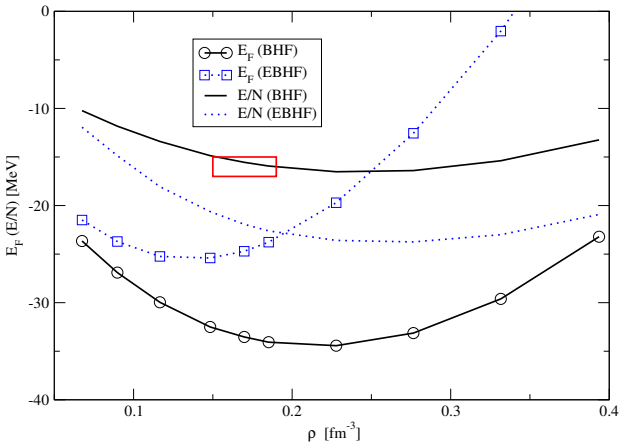

Fig. 3. The binding energy per particle calculated for Bonn C potential, using BHF (solid line) and EBHF (dotted line) as a function of density. The corresponding Fermi energies are denoted by the same lines with circles for BHF and squares for EBHF. The box describes the area in which nuclear saturation is expected to occur empirically.

matter compared to the corresponding T-matrix results from [18] using the CD-Bonn potential [32]. The T-matrix gives smaller binding energies and smaller Fermi energies than the BHF calculation. The repulsive effect increases with density. It can be assigned to the hh scattering contributions that are neglected in the BHF approximation. The relative importance of the hh scattering terms to the total energy grows, because the accessible space for the holes increases with increasing of the density. At low densities the BHF, EBHF and T-matrix results converge as expected. As we see from fig. 2, the Fermi energy obtained for different densities depends very much on the kind of chosen approximation. The EBHF and T-matrix are the Hugenholtz-Van Hove condition at the saturation point satisfied. As we see from fig. 2, there is excellent agreement between our calculations for binding energy using BHF approximation and Bożek's calculations [18] under the same approach (BHF).

For Bonn C [33] the EBHF is the Hugenholtz-Van Hove condition at the saturation point satisfied (fig. 3). The difference between $E_{\rm F}$ and $\frac{E}{N}$ at the saturation point is zero with numerical accuracy for the EBHF calculations (at saturation density $\rho_{\rm sat} = 0.195\,{\rm fm}^{-3}$ is $\frac{E}{N} = E_{\rm F} = -22.8\,{\rm MeV}$), and becomes as large as 18 MeV for the BHF approach. The saturation density for the EBHF is close to the empirical saturation density. It was argued in ref. [22] that the repulsive effect due to the inclusion of the hh scattering might be able to shift the saturation point close to the empirical value.

Stiff potentials like Bonn C [33], that are characterized by a strong repulsive core, usually saturated around the correct density, but do not produce enough binding energy, but their soft cores yield too dense systems (see table 1). In this way, an increase in binding energy is accompanied by an increase of the saturation density, as was first pointed out by Coester and collaborators [34].

Table 1. Saturation density, binding energy, Fermi energy and compression modulus for different approximations discussed in the text.

		$\rho_{\rm sat}$ (fm^{-3})	E/N (MeV)	$E_{\rm F}$ (MeV)	$K_{\rm nm}$ (MeV)
Bonn C	BHF	0.228	−16.52	−34.43	157.7
	EBHF	0.195	−22.8	−22.8	184
CD-Bonn	BHF	0.277	−22.86	−46.5	137.6
	EBHF	0.43	−27.8	−27.8	295

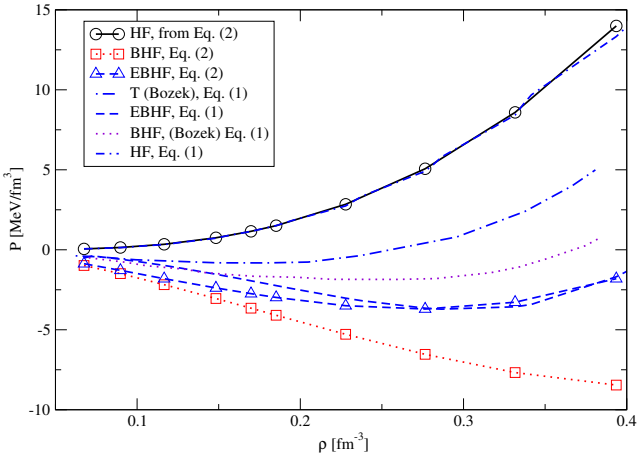

Fig. 4. Pressure as a function of density obtained from two different expressions, eqs. (1) and (2). The dash-dotted and the solid-with-circles lines represent the two results for the pressure in the HF calculation. The dotted-with-squares line represents the results in the BHF calculation. The dashed and the dashed-with-triangle-up lines represent the two results in the EBHF calculation. The dot-dashed line represents the T-matrix calculation from ref. [18]. The dotted line corresponds to the BHF calculation from ref. [18]. The results in this figure have been derived from the CD-Bonn interaction.

In table 1 are shown the corresponding binding energies and saturation densities for different approximations, using CD-Bonn and Bonn C potentials. The difference become as large as 23.6 MeV at $\rho_{\rm sat} = 0.277\,{\rm fm}^{-3}$ for the BHF approach, using the CD-Bonn potential.

The pressure can be calculated for a range of densities by two methods (eqs. (1) and (2)) which should be equivalent. However, only for the consistent approximation we find an approximate equivalence between the two formulae, with very good agreement for the Hartree-Fock calculation (figs. 4 and 5). The BHF violates badly the Hugenholtz-Van Hove relation for pressure at zero

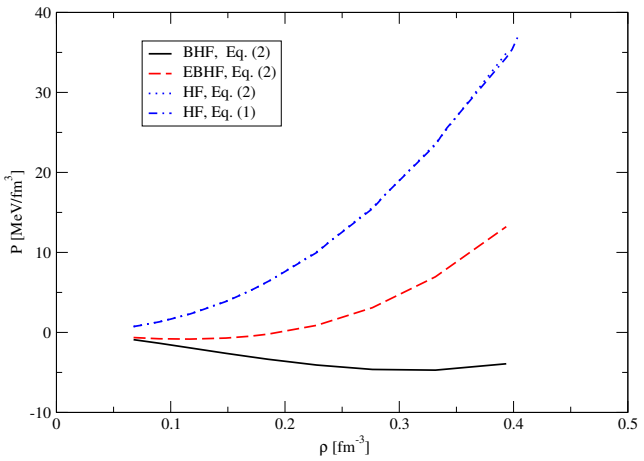

Fig. 5. Pressure obtained as a derivative of the binding energy, eq. (1), for the HF calculation (dash-dotted line) as a function of the density ρ. The corresponding pressures obtained using eq. (2) are denoted by dotted line for HF, solid line for BHF and dashed line for EBHF calculation, all for the Bonn C potential.

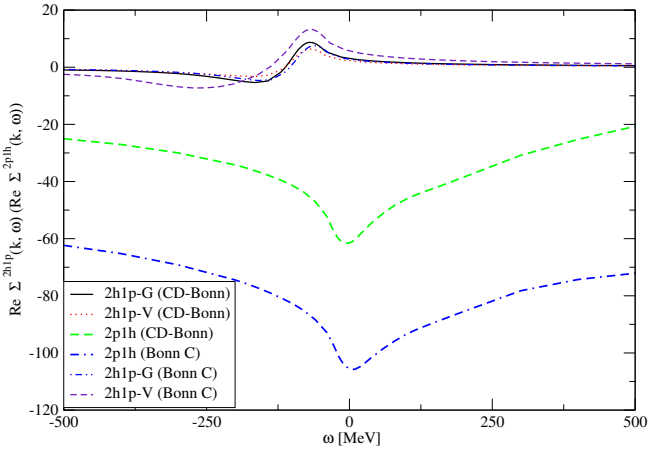

Fig. 6. The real part of the 2h1p (eqs. (6) and (7)) contribution to the self-energy as a function of ω evaluated for the CD-Bonn and Bonn C potentials assuming $k_{\rm F} = 1.36\,{\rm fm}^{-1}$ and momentum $k = 0.9k_{\rm F}$. For the sake of comparison, the self-energy for 2p1h is plotted in the same figure. Results are displayed for 2h1p from eq. (6) for CD-Bonn potential (solid line), 2h1p from eq. (7) for CD-Bonn potential (dotted line), for 2p1h for CD-Bonn potential (dashed line), for 2p1h for Bonn C potential (dash-dotted line), for 2h1p from eq. (6) for Bonn C (dot-dashed line) and for 2h1p from eq. (7) for Bonn C potential (dashed line).

temperature. The disagreement is reduced but not cured completely when using EBHF approach.

The slope of the pressure as a function of density defines the compression modulus of nuclear matter

$$K_{\rm nm} = 9\frac{\partial P}{\partial \rho}\,, \qquad (14)$$

which should be positive at the saturation point as a condition of stability. The nuclear-matter compression modulus is an important quantity in astrophysics and heavy-ion physics. The values of $K_{\rm nm}$ obtained in the different approaches using CD-Bonn and Bonn C potentials are shown in table 1. We find that, at the saturation point using EBHF, $K_{\rm nm} = 184\,{\rm MeV}$ for Bonn C. A recent analysis of the giant monople resonance in heavy nuclei [35] yields an experimental estimate for the compression modulus, $K_{\rm nm} = 210 \pm 30\,{\rm MeV}$. For Bonn C interaction the compression modulus obtained in EBHF agrees reasonably well with this value. For CD-Bonn potential and using EBHF approach, the value of $K_{\rm nm}$ obtained is larger than in usual nuclear matter because the saturation point is more than twice the empirical saturation density. The Gent group [22,36] finds that at the saturation point using the (continuous choice) BHF, $K_{\rm nm} = 154\,{\rm MeV}$ for Reid93 and $K_{\rm nm} = 148\,{\rm MeV}$ for the separable Paris potential. Also they found that $K_{\rm nm} = 177\,{\rm MeV}$ for Reid93 and $K_{\rm nm} = 216\,{\rm MeV}$ for separable Paris potential in the self-consistent treatment of short-range correlations.

Results for the 2h1p contribution to the self-energy, $\Sigma^{\rm 2h1p}$, are displayed in figs. 6 and 7. For comparison we have plotted the self-energy for 2p1h in the same figs. 6 and 7. In the first case we focus on the self-energy for 2h1p using G-matrix ($\Sigma_G^{\rm 2h1p}$ as in eq. (6)). In the second case the self-energy for 2h1p is calculated using bare potential ($\Sigma_v^{\rm 2h1p}$ as in eq. (7)). The imaginary part of $\Sigma^{\rm 2h1p}$ is different from zero only for energies ω below the Fermi energy, in case 2p1h is equal to zero below the Fermi energy. The conservation of the total momentum in the two-nucleon of the G-matrix in (6), $\mathbf{h}_1 + \mathbf{h}_2 = \mathbf{k} + \mathbf{p}_1$, leads to a minimal value of ω at which this imaginary part is different from zero. Due to these limitations, the imaginary part integrated over all energies is much smaller for $\Sigma^{\rm 2h1p}$ than for $\Sigma^{\rm 2p1h}$, displayed in the same figure. Since the imaginary part of $\Sigma^{\rm 2h1p}$ is significantly smaller than the one

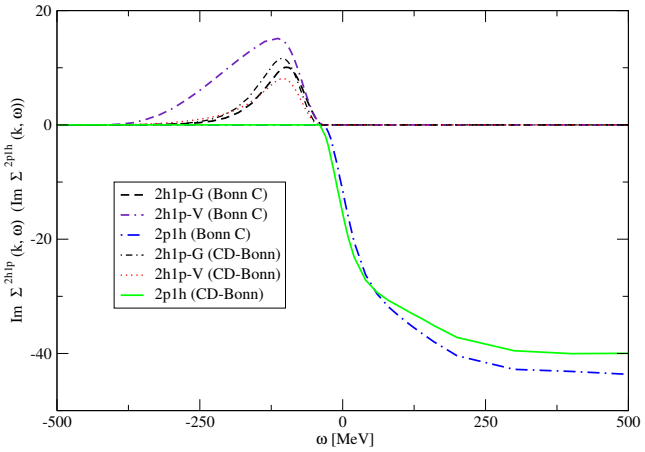

Fig. 7. Same as in fig. 6, but for the imaginary part.

of Σ^{2p1h}, the same is true also for the corresponding real part. The contribution of the hh term in the self-energy is smaller than the contribution of the pp term, so if one takes $G = v$ in the case of hh term, this will make a small shift in the results.

4 Conclusion

We have investigated the saturation of nuclear matter for different approximations using the CD-Bonn and Bonn C potentials. We find that the EBHF is conserving and fulfills the Hugenholtz-Van Hove relation.

I would like to thank Prof. Dr. H. Müther for useful discussions and guidance. Also I would like to thank Dr. M. Abdel-Aty for a critical reading of the manuscript.

References

1. H.S. Köhler, Phys. Rev. C **46**, 1687 (1992).
2. H.S. Köhler, R. Malfliet, Phys. Rev. C **48**, 1034 (1993).
3. T. Frick, Kh. Gad, H. Müther, P. Czerski, Phys. Rev. C **65**, 034321 (2002).
4. Kh. Gad, H. Müther, Phys. Rev. C **66**, 044301 (2002).
5. A. Ramos, A. Polls, W.H. Dickhoff, Nucl. Phys. A **503**, 1 (1989).
6. B.E. Vonderfecht, W.H. Dickhoff, A. Polls, A. Ramos, Nucl. Phys. A **555**, 1 (1993).
7. P. Bożek, Nucl. Phys. A **657**, 187 (1999).
8. J.P. Jeukenne, A. Lejeune, C. Mahaux, Phys. Rep. **25**, 83 (1976).
9. M. Baldo, F. Bombaci, G. Giansiracusa, U. Lombardo, C. Mahaux, R. Sartor, Phys. Rev. C **41**, 1748 (1990).
10. F. de Jong, R. Malfliet, Phys. Rev. C **44**, 998 (1991).
11. N.M. Hugenholtz, L. Van Hove, Physica **24**, 363 (1958).
12. J.M. Luttinger, J.C. Ward, Phys. Rev. **118**, 1417 (1960).
13. G. Baym, Phys. Rev. **127**, 1392 (1962).
14. V.F. Weisskopf, Nucl. Phys. **3**, 423 (1957).
15. H.A. Bethe, Phys. Rev. **103**, 1535 (1956).
16. P. Bożek, P. Czerski, Eur. Phys. J. A **11**, 271 (2001).
17. P. Bożek, Eur. Phys. J. A **15**, 325 (2002).
18. P. Bożek, P. Czerski, Acta. Phys. Pol. B **34**, 2759 (2003).
19. H.Q. Song, M. Baldo, G. Giansiracusa, U. Lombardo, Phys. Rev. Lett. **81**, 1584 (1998).
20. R.B. Wiringa, R.A. Smith, T.L. Ainsworth, Phys. Rev. C **29**, 1207 (1984).
21. B.D. Day, R.B. Wiringa, Phys. Rev. C **32**, 1057 (1985).
22. Y. Dewulf, W.H. Dickhoff, D. Van Neck, E.R. Stoddard, M. Waroquier, Phys. Rev. Lett. **90**, 152501 (2003).
23. W.H. Dickhoff, C. Barbieri, Prog. Part. Nucl. Phys. **52**, 377 (2004).
24. T. Frick, PhD Thesis, Tübingen University, (2004), unpublished.
25. E. Schiller, H. Müther, P. Czerski, Phys. Rev. C **59**, 2934 (1999); **60**, 059901 (1999)(E).
26. K. Suzuki, R. Okamato, M. Kohno, S. Nagata, Nucl. Phys. A **665**, 92 (2000).
27. M.I. Haftel, F. Tabakin, Nucl. Phys. A **158**, 1 (1970).
28. T. Cheon, E.F. Redish, Phys. Rev. C **39**, 331 (1989).
29. F. Sammarruca, X. Meng, E.J. Stephenson, Phys. Rev. C **62**, 014614 (2000).
30. P. Grange, J. Cugnon, A. Lejeune, Nucl. Phys. A **473**, 365 (1987).
31. C. Mahaux, R. Sartor, Adv. Nucl. Phys. **20**, 1 (1991).
32. R. Machleidt, F. Sammarruca, Y. Song, Phys. Rev. C **53**, R1483 (1996).
33. R. Machleidt, Adv. Nucl. Phys. **19**, 189 (1989).
34. F. Coester, S. Cohen, B. Day, C.M. Vincent, Phys. Rev. C **1**, 769 (1970).
35. J.P. Blaizot, J.F. Berger, J. Dechargé, M. Girod, Nucl. Phys. A **591**, 435 (1995).
36. Y. Dewulf, D. Van Neck, M. Waroquier, Phys. Rev. C **65**, 054316 (2002).